



Localized transition waves in bistable-bond lattices

L.I. Slepyan^{a,*}, M.V. Ayzenberg-Stepanenko^b

^a*Department of Solid Mechanics, Materials and Systems, Faculty of Engineering, Tel Aviv University,
P.O. Box 39040, Ramat Aviv 69978, Israel*

^b*Department of Mathematics, Ben Gurion University, P.O.Box 653, Beer-Sheva 84105, Israel*

Received 5 November 2003; received in revised form 28 January 2004; accepted 28 January 2004

Abstract

Discrete two-dimensional square- and triangular-cell lattices consisting of point particles connected by bistable bonds are considered. The bonds follow a trimeric piecewise linear force-elongation diagram. Initially, Hooke's law is valid as the first branch of the diagram; then, when the elongation reaches the critical value, the tensile force drops to the other. The latter branch can be parallel with the former (mathematically this case is simpler) or have a different inclination. For a prestressed lattice the dynamic transition is found analytically as a wave localized between two neighboring lines of the lattice particles. The transition wave itself and dissipation waves carrying energy away from the transition front are described. The conditions are determined which allow the transition wave to exist. The transition wave speed as a function of the prestress is found. It is also found that, for the case of the transition leading to an increased tangent modulus of the bond, there exists nondivergent tail waves exponentially localized in a vicinity of the transition line behind the transition front. The previously obtained solutions for crack dynamics in lattices appear now as a partial case corresponding to the second branch having zero resistance. At the same time, the lattice-with-a-moving-crack fundamental solutions are essentially used here in obtaining those for the localized transition waves in the bistable-bond lattices. Steady-state dynamic regimes in infinite elastic and viscoelastic lattices are studied analytically, while numerical simulations are used for the related transient regimes in the square-cell lattice. The numerical simulations confirm the existence of the single-line transition waves and reveal multiple-line waves. The analytical results are compared to the ones obtained for a continuous elastic model and for a related version of one-dimensional Frenkel–Kontorova model.
© 2004 Elsevier Ltd. All rights reserved.

Keywords: A. Dynamics; B. Phase transition; Bistable-bond lattice; C. Integral transforms

* Corresponding author. Tel.: +972-3640-6224; fax: +972-3640-7617.

E-mail addresses: leonid@eng.tau.ac.il, L.I.Slepyan@rogers.com (L.I. Slepyan).

1. Introduction

Two-dimensional lattices consisting of particles connected by massless bistable bonds are considered, Fig. 1. The bonds are assumed to obey a piecewise linear two-branch force-elongation relation, Fig. 2. At the transition point there exists a jump discontinuity in the tensile force. In addition, the branches may differ by the tangent modulus. Such a trimeric force-elongation diagram is characterized by five parameters: two moduli, two critical points (one is the transition point, the other is the limiting strain for the second branch) and the above-mentioned jump. Two of them can be taken as natural units, while remaining three parameters are important. This makes the bistable-bond lattice model essentially more general and suitable for the modelling of different two-dimensional phase transition and fracture processes. Here, we consider a localized transition wave.

If such a lattice is initially stressed, Fig. 2, it can behave as an active structure. As a result of a disturbance, it can release initially stored energy for the dynamic transition. In particular, the transition can arise as a *localized wave* propagating between two neighboring lines of the lattice particles. This wave results in the unloading of the outer bonds which thus remain in the initial phase. So, we face a one-dimensional transition wave propagating in a two-dimensional lattice. Note, however, that this localized transition wave is accompanied by the structure-associated sinusoidal waves excited by the transition front. These waves can carry energy away from the transition line.

Such a line transition wave looks like a propagating crack bridged by fibres as in fracture of fibre-reinforced composites (Budiansky et al., 1986; Willis, 1993; Meda and Steif, 1994a,b; Movchan and Willis, 1996, 1997a,b, 1998; Huang et al., 1999; Nemat-Nasser and Luqun, 2001; Biner, 2002).

The present formulation integrates those used (a) in works on one-dimensional phase transition waves in bistable chains (Slepyan and Troyankina, 1984, 1988; Puglisi and Truskinovsky, 2000; Slepyan, 2000, 2001b, 2002; Balk et al., 2001a,b; Charlotte and Truskinovsky, 2002; Ngan and Truskinovsky, 2002; Kresse and Truskinovsky, 2003, Kresse and Truskinovsky, 2004; Truskinovsky and Vainchtein, 2004; Cherkaev et al., 2004; Slepyan et al., 2004) and (b) in fracture of two-dimensional lattices (Slepyan, 1981, 2000, 2001a,c, 2002; Kulakhmetova et al., 1984; Fineberg et al., 1991, 1992; Marder and Liu, 1993; Marder and Gross, 1995; Kessler and Levine, 1998, 2001; Fineberg and Marder, 1999; Slepyan et al., 1999; Kessler, 2000; Gerde and Marder, 2001; Pechenik et al., 2002; Slepyan and Ayzenberg-Stepanenko, 2002).

A lattice model of the Peierls type is used in the recent work by Movchan et al. (2003). In this paper, a two-dimensional lattice is introduced as an interface embedded into a homogeneous three-dimensional elastic space. The motion of a dislocation kink is studied. The resulting integral equation is resolved numerically. Also, a finite-thickness structural interface consisting of several lattice layers is considered for a homogeneous two-dimensional elastic body.

It should be mentioned that active lattices of different nature, as networks of identical or almost identical interacting units ordered in space, are considered in many works based on a synergetic approach, see Nekorkin and Velarde (2002). Theoretical methods

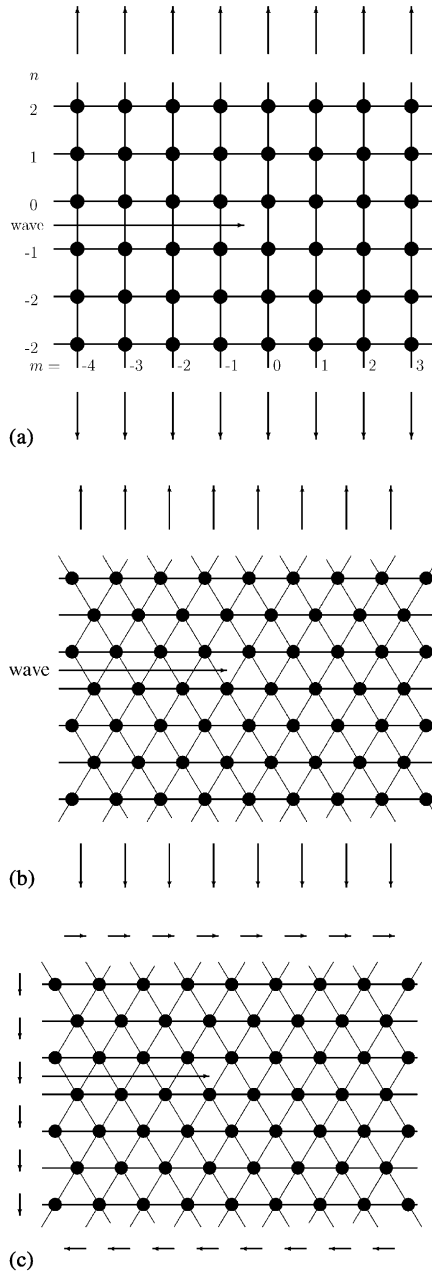


Fig. 1. The lattices: (a) Square-cell lattice. It is intended to model anti-plane shear (mode III); however, a hypothetical plane deformation with only vertical displacements—with the same formulation and results—can also be assumed. The latter viewpoint is used when it is more convenient; for example, when displacements and forces are shown in a plane figure. (b) Triangular-cell lattice under mode I extension. (c) Triangular-cell lattice under mode II shear.

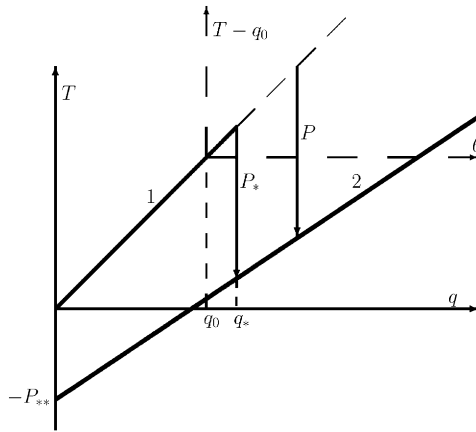


Fig. 2. Force-elongation diagram: (1) the first, initial branch; it corresponds to the initial phase characterized by a unit nondimensional stiffness, $T = q$. (2) The second branch, $T = q - P_* - (1 - \gamma)(q - q_*) = -P_{**} + \gamma q$; it comes in force when the elongation reaches the critical value, $q = q_*$. The vertical distance between the branches is denoted by P . This phase transition is assumed irreversible. The dotted axes correspond to the diagram plotted relatively the initial state where the elongation of nonhorizontal bonds is equal to q_0 . This latter diagram is used when the problem is formulated with respect to the dynamic elongation additional to the initial static state. Initial elongation of the horizontal bonds is at zero or negative and, in the analytical formulation, they are assumed to be in the initial phase all the time not to suffer the phase transition.

of the qualitative theory of dynamical systems, and numerical simulations are used. One-dimensional transition waves are shown.

In the present work, the Fourier transform and the Wiener–Hopf technique are used allowing the detailed solution for a two-dimensional problem to be obtained including that for the structure of the radiation (dissipation) during the moving transition. This becomes possible for discrete square- and triangular-cell lattices with bistable bonds characterized by piecewise linear (trimeric) stress–strain dependencies. Related transient problems are considered numerically. The analytical results are compared to the ones obtained for a continuous elastic model and for a related version of one-dimensional discrete Frenkel–Kontorova model (Frenkel and Kontorova, 1938).

The goal of the present study is to determine the conditions allowing such a transition wave to arise, and its speed as a function of the initial stress which defines the energy release rate during the dynamic transition. In a special case, where the phases differ only by a jump in the tensile force, while the tangent modulus is the same for both branches, the bonds are assumed elastic or viscoelastic (the model of a standard viscoelastic material is used). In a general case, only elastic bistable lattices are considered.

Previously obtained solutions for crack dynamics in lattices appear now as a partial case corresponding to the second branch having a zero resistance. At the same time, the lattice-with-a-moving-crack fundamental solutions are essentially used here in obtaining those for the localized transition waves in the bistable-bond lattices. This allows us to avoid the need to consider and to solve the lattice dynamic equations; we thus avoid the associated complicated conversions.

Square- and triangular-cell lattices are examined. Note that the square-cell lattice is intended to model anti-plane shear; however, a hypothetical plane deformation with only vertical displacements—with the same formulation and results—can also be assumed. We use the latter viewpoint when it is more convenient; for example, when displacements and forces are to be shown in a plane figure.

2. Formulation

Consider a lattice, Fig. 1, consisting of point particles each of mass M connected by massless bistable bonds which obey the force-elongation relation

$$\begin{aligned}
 T = q \quad (t < t_*), \quad T = q - P_* - (1 - \gamma)(q - q_*) = \gamma q - P_{**} \quad (t > t_*), \\
 P_{**} = P_* - (1 - \gamma)q_*, \quad q < q_* \quad (t < t_*), \quad q = q_* \quad (t = t_*)
 \end{aligned} \tag{1}$$

shown in Fig. 2. Here T and q are the nondimensional tensile force and elongation, t_* is the moment of time, t , when the elongation first reaches the critical value, q_* . At this moment the transition occurs from the first branch of the diagram in Fig. 2 to the other, lower branch whose nondimensional tangent modulus is equal to γ ; P_* is the vertical distance between the branches at $q = q_*$, while P_{**} is that at $q = 0$. Here and below we use the nondimensional values as

$$\begin{aligned}
 u'_m = \frac{u_m}{a}, \quad v' = \frac{v}{c}, \quad t' = \frac{ct}{a}, \quad x' = \frac{x}{a}, \quad y' = \frac{y}{a}, \\
 q'_m = \frac{q_m}{a} = u'_m - u'_{m-1}, \quad T' = \frac{T}{\mu a}, \quad P'_* = \frac{P_*}{\mu a}
 \end{aligned} \tag{2}$$

(but with the superscript dropped) for the displacements, the transition wave speed, time, rectangular coordinates, elongations, the tensile force and the jump discontinuity in the force-elongation diagram, respectively; $c = a\sqrt{\mu/M}$, a and μ are the characteristic speed, the bond length and the first branch tangent modulus, respectively. The x, y coordinate origin is taken at $m = n = 0$, where n is the particle line number. So, the particle coordinates at $n = 0$ ($y = 0$) are $x = 0, \pm 1, \dots$. For the square-cell lattice this is valid for any n , while for the triangular-cell lattice those are defined as $x = n/2 + m$.

Recall that for $t < t_*$ the bond is in the initial phase characterized by a unit nondimensional stiffness. The phase transition occurs at $t = t_*$ when the elongation first reaches the critical value, q_* . At this moment a jump in the tensile force arises, $[T] = T(t_* + 0) - T(t_* - 0) = -P_* \leq 0$, and the bond comes into the other phase where the tangent modulus $dT/dq = \gamma$. Note that the phase transition moment, $t = t_*$, is different for different bonds. A one-dimensional elastic chain with such an irreversible behavior of its bonds is considered in Slepyan et al. (2004). A partial case of two linear branches for the chain, $T = q$ and $T = \gamma q$ ($\gamma < 1$) was examined in Slepyan and Troyankina (1984), while the case $P_* < 0, \gamma > 1, P_{**} > 0$, also for the chain, was studied in Slepyan and Troyankina (1988). A reversible two-phase chain was considered by Balk et al. (2001a,b).

Initially, the lattice is assumed to be uniformly stressed in such a way that the elongation of the y -directed or inclined bonds (as in a square-cell or in a triangular-cell

lattice, respectively), q_0 , is below the critical value, q_* . The x -directed bonds are not stressed (this corresponds to mode I unidirectional strain of the lattice and to modes II and III), or these bonds are slightly compressed (as in the case of mode I unidirectional stress of the lattice). Note that in the case of mode II for the triangular-cell lattice, lengthening and shortening of the inclined bonds alternate. In this case, the critical value is assumed to be $\pm q_*$ for these deformations, respectively.

For the analytical analysis it is reasonable to assume that the phase transition wave arising from a small disturbance is localized between the neighboring lines of particles (denoted as $n = 0$ and -1). Indeed, the negative jump in the tensile force acts to unload the y -directed or inclined bonds outside this damaged band, while the initially unstressed x -directed bonds have a great safety factor. (The results of numerical simulations discussed below show when the localized transition wave can exist.) It is also assumed that the wave propagates with a constant speed v . This means that the time-interval between the transformation of the neighboring bonds is $1/v$ for the square-cell lattice and $1/(2v)$ for the triangular-cell lattice (see Fig. 1). Under these conditions, the steady-state regime is considered with the transformed-bond region at $\eta = x - vt < 0$.

Thus, we face a steady-state problem for a lattice whose bonds are in the initial phase except those placed between lines $n = 0$ and -1 at $\eta < 0$ where the bonds are in the second phase. The solution is required that satisfies the dynamic equations for such a ‘damaged’ lattice and the following inhomogeneous conditions at infinity: the strain field coincides with a given initial one at $y = \pm\infty$ and $\eta = +\infty$. The solution presents the elongation of a bond at the moment of the above-mentioned transformation, $\eta = 0$, as a function of the wave speed, v , and the initial elongation. The equality

$$q(\eta) = q_* \quad (\eta = 0) \quad (3)$$

serves for the determination of the speed as a function of the initial elongation. In addition, the solution must satisfy the admissibility condition

$$q < q_* \quad (\eta > 0). \quad (4)$$

Otherwise, the transition occurs earlier, that is, the transition wave speed is really greater than in the solution, in spite of the fact that the condition (3) is satisfied (for fracture this was pointed out by Marder and Gross, 1995). In addition, for a single-line transition wave the condition in (4) must be satisfied outside the transition layer. This point will be discussed in Section 4.7.

For our goal it is convenient to reformulate this problem as follows. Consider a uniform lattice all the bonds of which are in the initial phase for any q . Introduce self-equilibrated pairs of external forces applied to the particles connected by the transition-line bonds. The forces are directed along the corresponding bond as shown in Fig. 3. Referring to (1) choose the forces as

$$P(\eta) = P_* + (1 - \gamma)[q(\eta) - q_*] \quad (\eta < 0), \quad P(\eta) = 0 \quad (\eta \geq 0). \quad (5)$$

The intact bonds together with these external forces act on the transition-line particles, $n = 0$ and $n = -1$, in the same way as if the bonds are in the second phase. Hence, such a reformulation does not influence the lattice dynamic behavior.

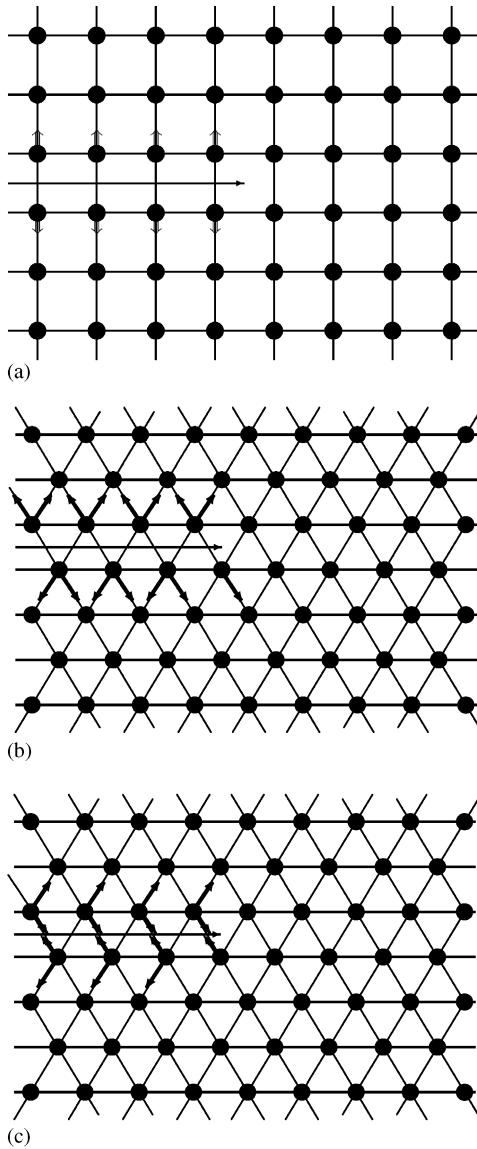


Fig. 3. Phase transition in a band modelled by self-equilibrated external forces. All the bonds of the lattice are assumed to be in the initial phase, but those between the particle lines $n=0$ and -1 at $\eta < 0$ ($t > m/v$) are loaded by the forces, $P=P_*(1-\gamma)(q-q_*)$, as shown in this figure. For the lattice particle dynamics this is the same as if those bonds are in the other phase. (a) The square-cell lattice (see the caption for Fig. 1). (b) Mode I triangular-cell lattice. (c) Mode II triangular-cell lattice.

We now consider the problem for $P_* > 0$, $\gamma \geq 0$ ($P_* < q_* - q_0$ if $\gamma=0$). The limiting partial case

$$P_* = q_*, \quad q_0 = \gamma = 0 \tag{6}$$

corresponds to a free-face crack considered in Slepyan (2001a, c, 2002). Another remarkable case, $\gamma=1$, will be considered separately and also as the limiting case ($\gamma \rightarrow 1$) of the solution corresponding to $\gamma \neq 1$.

3. Governing equation for elastic lattices

To proceed we introduce a steady-state fundamental solution, $Q(\eta)$, as the elongation of the bonds between lines $n = 0$ and -1 caused by the external self-equilibrated pair of impulsive forces $P = \delta(\eta)$, Fig. 4. In the case of mode II, these forces act to stretch the right-inclined bonds and to compress the left-inclined bonds. For other modes these forces act on each bond equally. In these terms, the additional elongation of a transition-line bond caused by a general distribution of external forces, $P(\eta)$, is

$$\theta(\eta) = q(\eta) - q_0 = Q(\eta) * P(\eta), \tag{7}$$

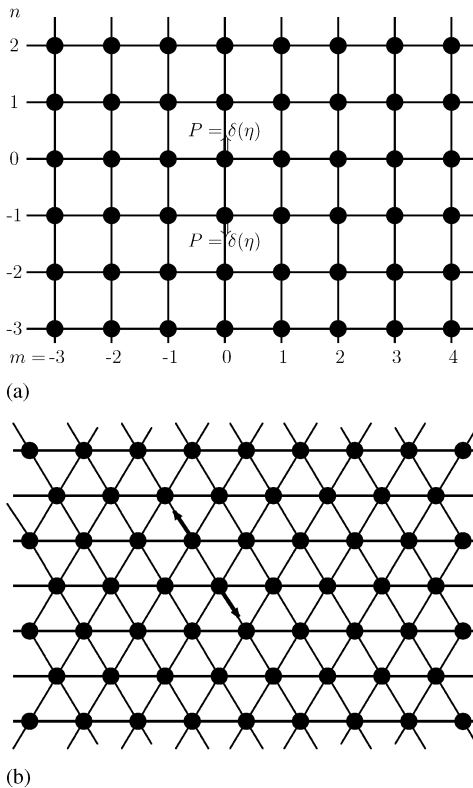


Fig. 4. External forces corresponding to the fundamental solution for an intact lattice: (a) Square-cell lattice; (b) Triangular-cell lattice.

where $*$ is the convolution symbol. In terms of the Fourier transform, this equality becomes

$$\theta^F(k) = Q^F(k)P^F(k). \tag{8}$$

We now denote

$$\theta^F = \theta_+ + \theta_-, \quad \theta_{\pm} = \int_{-\infty}^{\infty} \theta(\eta)H(\pm\eta)e^{ik\eta} d\eta, \tag{9}$$

where H is the Heaviside unit step function. The same subscript, $+$ ($-$), will be used for the right-side (left-side) Fourier transform of any function. Referring to Eq. (5)

$$P^F = P_- = P_*(0 + ik)^{-1} + (1 - \gamma)[\theta_- - \theta_*(0 + ik)^{-1}], \tag{10}$$

where $\theta_* = q_* - q_0$. Note that the symbol $0 + ik$ means $\lim(s + ik)$, $s \rightarrow +0$, that reflects here the generalized Fourier transform. Eq. (8) can now be represented in the form

$$\theta_+ + [1 - (1 - \gamma)Q^F]\theta_- = [P_* - (1 - \gamma)\theta_*] \frac{Q^F}{0 + ik}. \tag{11}$$

Fortunately, to find the function $Q^F(k)$ appearing in this equation we have no need to consider the corresponding dynamic problem for the lattices. Since it is defined for the intact lattice, that is, it is independent of the parameters P_*, q_0, γ , it can be expressed in terms of the known lattice-with-a-crack Green function denoted by $L(k)$ in Slepyan (2002). With this in mind we rearrange relation (7) to obtain the corresponding equation for the lattice with a crack at $\eta < 0$. Represent

$$P^F(k) = q_-(k) + p^F(k), \tag{12}$$

where $p(\eta)$ is an arbitrary function, and put $q_0 = 0$. The first term in the right-hand side of Eq. (12) compensates the tensile forces in the considered bonds at $\eta < 0$ and hence, as far as the external forces are defined by Eq. (12), this corresponds to a lattice with a crack at $\eta < 0$ loaded at $n = 0$ and -1 by the self-equilibrated pairs of forces, $p(\eta)$.

In the considered case $\theta(\eta) = q(\eta)$ and Eq. (8) leads to

$$L(k)q_+(k) + q_-(k) = [L(k) - 1]p^F \tag{13}$$

with

$$L(k) = [1 - Q^F]^{-1}. \tag{14}$$

In terms of the elongations, Eq. (13) coincides with the governing equations for crack dynamics [see Eqs. (11.16) and (12.4) in Slepyan (2002), where the elongation is denoted by capital Q , $u = Q/2$ and the external forces are denoted by q]. Thus, the expressions for $L(k)$ presented in this book [Eqs. (11.17) and (12.47)] can be used to find Q^F from (14). It follows that

$$Q^F = 1 - \frac{1}{L(k)}, \tag{15}$$

where for mode III unbounded square-cell lattice

$$L(k) = \sqrt{\frac{r(k)}{h(k)}} \tag{16}$$

with

$$h(k) = 2(1 - \cos k) + Y,$$

$$r(k) = h(k) + 4 \tag{17}$$

and

$$Y = (0 + ikv)^2, \quad 0 + ikv = \lim_{s \rightarrow +0} (s + ikv). \tag{18}$$

Note that the latter limit reflects the causality principle for steady-state solutions (see Slepyan, 2002). The function $L(k)$ for a square-cell lattice strip can be found in Slepyan et al. (1999) and Slepyan (2002).

For a triangular-cell lattice

$$L(k) = \frac{r_A(k)}{h_A(k)}, \tag{19}$$

where

$$h_A = \frac{F(n_2)\sqrt{n_1^2 - 1} - F(n_1)\sqrt{n_2^2 - 1}}{n_2 - n_1}, \quad r_A = 3\sqrt{n_1^2 - 1}\sqrt{n_2^2 - 1},$$

$$F(n_{1,2}) = 3(\cos k/2 - n_{1,2})^2 + 6 \sin^2 k/2(1 \pm \cos k/2)(1 \mp n_{1,2})$$

$$+ Y[(1 \pm \cos k/2)(1 \mp n_{1,2}) + 1 - n_{1,2} \cos k/2]. \tag{20}$$

In the expression for $F(n_{1,2})$, upper signs correspond to mode I, while lower signs correspond to mode II. Functions $n_{1,2}$ are

$$n_{1,2} = \left(1 + 2 \sin^2 k/2 + \frac{2}{3} Y \right) \cos k/2$$

$$\mp \left[\frac{1}{9} Y^2 - 4 \sin^2 \frac{k}{2} \left(\sin^2 \frac{k}{2} + \frac{1}{3} Y \right)^2 \right]^{1/2}. \tag{21}$$

The rule of the determination of signs of the radicals in the above relations [the argument of a radical is continuous in a pre-limiting case, $s > 0$, see Eq. (18)], as well as the asymptotes for $k \rightarrow 0$ and $k \pm \infty$, can be obtained from the corresponding sections of the book by Slepyan (2002). In particular,

$$\frac{h(k)}{r(k)} \rightarrow \frac{h_A(k)}{r_A(k)} \rightarrow 1 \quad (k \rightarrow \pm\infty). \tag{22}$$

Eq. (11) can now be rewritten as

$$\mathcal{L}(k)\theta_+ + \theta_- = \frac{q^0[\mathcal{L}(k) - 1]}{0 + ik} \tag{23}$$

with

$$q^0 = \frac{P_{**}}{1 - \gamma}, \quad P_{**} = P_* - (1 - \gamma)\theta_* \tag{24}$$

and

$$\mathcal{L}(k) = \frac{L(k)}{\gamma L(k) + 1 - \gamma}. \tag{25}$$

Note that the initial strain does not appear in the governing equation (23). The problem may thus be considered in terms of the additional elongations vanishing at $x \rightarrow +\infty$ and $y \rightarrow \pm\infty$, as if the force-elongation diagram has its origin at $q=q_0, T=q_0$ as shown in Fig. 2.

4. Solution for $\gamma \neq 1$

4.1. Derivation of main relations

Eq. (23) can be solved using the Wiener–Hopf technique. In this connection first note some features of the function $L(k)$ in Eq. (25). Under the causality principle this function should be considered as the limit ($s \rightarrow +0$) of $L(s+ikv, k)$ (see Slepyan, 2002); further we denote this function $L(k)$. It follows from the *Theorem of the fundamental solution* (Slepyan, 2001c, 2002) that if $s > 0$, as k runs over the real axis from $-\infty$ to ∞ , the function $L(k)$ forms a closed contour in the complex plane, $\Re L(k) + i\Im L(k)$, leaving the negative half-axis, $\Re L(k) \leq 0$, in the outer domain. This evidences that

$$\text{Ind } L(k) = \frac{1}{2\pi} [\text{Arg } L(\infty) - \text{Arg } L(-\infty)] = 0. \tag{26}$$

It follows that the denominator in Eq. (25), $\gamma L(k) + 1 - \gamma$, possesses the same features at least for $0 \leq \gamma \leq 1$. Hence, in this range of γ

$$\text{Ind } \mathcal{L}(k) = 0. \tag{27}$$

In fact, this equality is valid for any value of $\gamma > 0$. Indeed, we have

$$\text{Ind } \mathcal{L}(k) = \text{Ind } L(k) - \text{Ind}[1 - \gamma + \gamma L(k)] \tag{28}$$

with $\text{Ind } L(k) = 0$. In its turn,

$$L(k) = 1 - \mu U^{\text{LF}}(s' + ikv, k), \tag{29}$$

where $U(t, \eta)$ is the fundamental solution for the lattice half-plane [see Eq. (12.13) in the book by Slepyan, 2002]. The theorem on the fundamental solution presented there states that *If $s' > 0$, the double, Laplace (on t) and Fourier (on η) transform of the solution, U^{LF} , cannot be positive for any k .* As a consequence

$$1 - \gamma + \gamma L(k) = 1 - \gamma \mu U^{\text{LF}} \not\leq 0 \quad (s' > 0). \tag{30}$$

At the same time,

$$1 - \gamma + \gamma L(k) = 1 \quad (k = \pm\infty). \tag{31}$$

It follows that when k runs from $-\infty$ to ∞ this function forms a closed contour in the complex plane, while the origin, $k = 0$, is outside this contour. Thus, for any $\gamma > 0$

$$\text{Ind}[1 - \gamma + \gamma L(k)] = \text{Ind } \mathcal{L}(k) = 0. \tag{32}$$

Further, $L(\pm\infty) = 1$ and it can be seen in Eq. (25) that this equality is still valid for $\mathcal{L}(k)$. The function $\mathcal{L}(k)$ can thus be factorized using the Cauchy-type integral, namely

$$\begin{aligned} \mathcal{L}(k) &= \mathcal{L}_+ \mathcal{L}_-, \\ \mathcal{L}_\pm &= \exp \left[\pm \frac{1}{2\pi i} \int_{-\infty}^{\infty} \frac{\ln \mathcal{L}(\xi)}{\xi - k} d\xi \right], \end{aligned} \tag{33}$$

where $\Im k > 0$ for \mathcal{L}_+ and vice versa. If $s > 0$ the function $\mathcal{L}_+(k)$ [$\mathcal{L}_-(k)$] has no zeros and singular points in the upper (lower) half-plane with the real axis. In particular, it follows that

$$\mathcal{L}_+ \rightarrow 1 \quad (k \rightarrow i\infty), \quad \mathcal{L}_- \rightarrow 1 \quad (k \rightarrow -i\infty). \tag{34}$$

Noting that $\mathcal{L}(0) = 1/\gamma$ [$L(0) = \infty$] we now can rearrange Eq. (23) in the form

$$\begin{aligned} \mathcal{L}_+(k)\theta_+ + \frac{\theta_-}{\mathcal{L}_-(k)} &= \frac{q^0[\mathcal{L}_+(k) - 1/\mathcal{L}_-(k)]}{0 + ik} = C_+(k) + C_-(k), \\ C_+(k) &= \frac{q^0[\mathcal{L}_+(k) - \mathcal{L}_+(0)]}{0 + ik} = \frac{q^0[\mathcal{L}_+(0) - \mathcal{L}_+(k)]}{0 - ik}, \\ C_-(k) &= \frac{q^0[\mathcal{L}_+(0) - 1/\mathcal{L}_-(k)]}{0 + ik}, \\ \mathcal{L}_\pm(0) &= \frac{1}{\sqrt{\gamma}} \mathcal{R}^{\pm 1}, \quad \mathcal{R} = \exp \left[\frac{1}{\pi} \int_0^\infty \frac{\text{Arg } \mathcal{L}(\xi)}{\xi} d\xi \right]. \end{aligned} \tag{35}$$

The functions $C_+(k)$ and $C_-(k)$ have no singular points in the upper and lower half-planes, respectively [point $k = 0$ is regular for C_+ ; this allows us to change $0 + ik$ to $-(0 - ik)$]. Now, following the Wiener–Hopf technique and taking into account the condition $\theta = 0$ at $\eta = +\infty$, we can simply separate the corresponding functions in Eq. (35) and find the solution as

$$\theta_+(k) = \frac{C_+(k)}{\mathcal{L}_+(k)}, \quad \theta_-(k) = C_-(k)\mathcal{L}_-(k). \tag{36}$$

For $\eta = 0$ Eq. (36) yields

$$\begin{aligned} \theta(0) &= \lim_{p \rightarrow \infty} p\theta_+(ip) = \lim_{p \rightarrow \infty} p\theta_-(-ip) = q^0[\mathcal{L}_+(0) - 1] \\ &= q^0 \left(\frac{1}{\sqrt{\gamma}} \mathcal{R} - 1 \right). \end{aligned} \tag{37}$$

In the considered wave, if it exists, $\theta(0) = \theta_*$. This results in the following equation:

$$\mathcal{R} = \sqrt{\gamma} \left(\frac{\theta_*}{q^0} + 1 \right) = \frac{\sqrt{\gamma} P_*}{P_* - (1 - \gamma)\theta_*}. \tag{38}$$

This equation defines the transition wave speed [\mathcal{R} is defined in Eq. (35) as a function of v]. If no wave speed satisfies this equation the wave does not exist. Solution (36) can thus be rewritten as

$$\begin{aligned} \theta_+(k) &= \left[\frac{P_*}{1 - \gamma} \left(\frac{1}{\mathcal{L}_+(k)} - 1 \right) + \theta_* \right] \frac{1}{0 - ik}, \\ \theta_-(k) &= \left[\frac{P_*}{1 - \gamma} (\mathcal{L}_-(k) - 1) + \theta_* \right] \frac{1}{0 + ik}. \end{aligned} \tag{39}$$

4.2. The elongation at infinity

The limits of $\theta(\eta)$ for $\eta \rightarrow \pm\infty$ follow from Eq. (36) [also see Eqs. (23) and (35)] as

$$\begin{aligned} \theta(+\infty) &= \lim_{p \rightarrow 0} p\theta_+(ip) = 0, \\ \theta(-\infty) &= \lim_{p \rightarrow 0} p\theta_-(-ip) = \frac{P_{**}}{\gamma} \end{aligned} \tag{40}$$

as they should be. They are the static elongation corresponding to the first phase at $\eta \rightarrow +\infty$ and to the second phase at $\eta \rightarrow -\infty$.

4.3. The energy release and the transition wave speed

The phase transformation path on the ‘macrolevel’, that is, in the long-wave approximation where no high-frequency dissipative waves are detected, corresponds to the horizontal segment presented in Fig. 5. Triangle CDE represents the released energy a part of which is spent in overcoming the energy barrier (triangle ABC). The resulting energy released on the macrolevel per bond, is thus represented by the difference of the areas of the latter and former triangles. As can be seen in Fig. 5 the nondimensional energy release per bond is

$$G = \frac{1}{2\gamma} (P_* - \theta_*)^2 - \frac{1}{2} \theta_*^2. \tag{41}$$

The energy dissipation per unit time is vG for the square-cell lattice and $2vG$ for the triangular-cell lattice. In terms of the total energy release rate,

$$\theta_* = \frac{P_*}{\sqrt{\gamma}\sqrt{1 + 2G^0} + 1} \quad \left(G^0 = \frac{G}{\theta_*^2} \right) \tag{42}$$

and Eq. (38) can be rewritten in the form

$$\mathcal{R} = \frac{1 + \sqrt{\gamma}\sqrt{1 + 2G^0}}{\sqrt{\gamma} + \sqrt{1 + 2G^0}}. \tag{43}$$

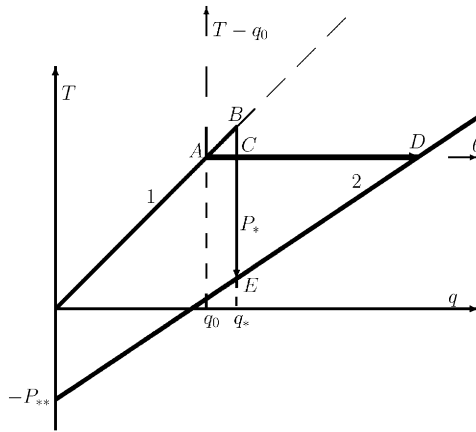


Fig. 5. Phase transition path on the macrolevel and the energy release. The phase transition path is shown by arrow AD on the θ -axis. Triangle CDE represents the released energy a part of which is spent for overcoming the energy barrier (triangle ABC), while the rest part is radiated away from the transform band with sinusoidal waves. The resulting energy released on the macrolevel per bond, is represented by the difference of the areas of the latter and former triangles.

This equation defines the speed as a function of G^0 . It can be observed that

$$\mathcal{R} = 1 \quad (G^0 = 0), \quad \mathcal{R} = \sqrt{\gamma} \quad (G^0 = \infty),$$

$$\frac{d\mathcal{R}}{dG^0} < 0 \quad (\gamma < 1), \quad \frac{d\mathcal{R}}{dG^0} > 0 \quad (\gamma > 1). \tag{44}$$

The inverse relation is

$$G^0 = \frac{1}{2} \left[\left(\frac{1 - \mathcal{R}\sqrt{\gamma}}{\mathcal{R} - \sqrt{\gamma}} \right)^2 - 1 \right]. \tag{45}$$

In accordance with the obtained solution, this energy is radiated away from the transition front with sinusoidal dissipative waves. The nonzero real singular points of $\theta_{\pm}(k)$ are their wavenumbers. They can be specified as follows. Square-root-type real singular points of $\mathcal{L}_+(k)$ [in Eq. (39) for $\theta_+(k)$] are zeros of $h(k)$ and $g(k)$ of the type $k = k_{\mu} - i0$. These points represent waves propagating ahead of the transition front. Real singular points of $\mathcal{L}_-(k)$ [in Eq. (39) for $\theta_-(k)$] are zeros of $h(k)$ and $g(k)$ of the type $k = k_{\nu} + i0$. The corresponding waves propagate behind the front.

For $v > 0$ there exist a finite number of such points; the number increases as the speed decreases. Note that the obtained solution directly defines these waves only in the considered layer of the bonds. In fact, the sinusoidal waves carry energy away from the transition layer to the bulk of the lattice, and their amplitudes decrease with the distance from the transition front due to geometrical divergence. (In this connection, see Sections 11.5.5 and 11.5.6 in the book by Slepyan, 2002.)

In addition, if $\gamma > 1$, there exist simple or multiple poles of $\mathcal{L}_-(k)$ as zeros of $\gamma\mathcal{L}(k) + 1 - \gamma$ of the type $k = k_{\nu} + i0$. The corresponding waves do not diverge. We now study such a remarkable *tail wave* in more detail.

4.4. Localized sinusoidal waves in an infinite lattice

Consider an infinite square-cell lattice whose bonds between lines $n=0$ and $n=-1$ are in the second phase, while others are in the first phase. If this lattice is at rest, its equilibrium state corresponds to that far behind the transition front (see Section 4.2). In terms of additional displacements, the dynamic equations are

$$\begin{aligned} \ddot{u}_{m,n}(t) &= u_{m-1,n}(t) + u_{m+1,n}(t) \\ &+ u_{m,n-1}(t) + u_{m,n+1}(t) - 4u_{m,n}(t) \quad (n \geq 1, n \leq -2), \\ \ddot{u}_{m,0}(t) &= u_{m-1,0}(t) + u_{m+1,0}(t) + u_{m,1}(t) - 3u_{m,0} + \gamma[u_{m,-1}(t) - u_{m,0}(t)], \\ \ddot{u}_{m,-1}(t) &= u_{m-1,-1}(t) + u_{m+1,-1}(t) + u_{m,-2}(t) - 3u_{m,-1} \\ &+ \gamma[u_{m,0}(t) - u_{m,-1}(t)]. \end{aligned} \tag{46}$$

We seek the solution in the form

$$\begin{aligned} u_{m,n}(t) &= \lambda^n \exp[ik(m - vt)] \quad (n \geq 0), \\ u_{m,n}(t) &= -\lambda^{1-n} \exp[ik(m - vt)] \quad (n \leq -1) \end{aligned} \tag{47}$$

with $|\lambda| < 1$, that is, a solution vanishing as $n \rightarrow \pm\infty$ and having symmetry related to the transition wave problem. Substituting this in the first of Eqs. (46) we obtain two possible solutions characterized by

$$\lambda = \lambda_{1,2} = \frac{1}{2} [h(k) + 2] \pm \sqrt{\frac{1}{4}[h(k) + 2]^2 - 1} \quad \left(\lambda_2 = \frac{1}{\lambda_1} \right). \tag{48}$$

We now substitute any of them in the second equation (or, equivalently, in the third one). It follows that

$$\lambda \left(-\frac{1}{\lambda} - 2\gamma + 1 \right) = 0 \Rightarrow \lambda = -\frac{1}{2\gamma - 1}. \tag{49}$$

So, solution (47) with $|\lambda| < 1$ can exist only if $\gamma > 1$; it corresponds to $\lambda = \lambda_1$. For $\gamma < 1$ an exponentially growing wave exists, $|\lambda| > 1$, while for $\gamma=1$ the wave represents constant amplitude antiphase oscillations.

Note that, in the considered phase transition problem, waves with $|\lambda| > 1$ cannot be excited at all, the uniform wave gradual formation occurs due to the radiation of a divergent wave, and only the exponentially decreasing waves, $|\lambda| < 1$, having a finite energy density per unit length can exist behind the transition front. In the η -uniform lattice considered in this section, such a wave carries energy along the higher-modulus layer and represents thickness (antiphase) oscillations whose amplitude exponentially decreases as $|n|$ increases. Note that this is a genuine lattice solution having no analogue in the corresponding continuous model.

From Eq. (48) it now follows that

$$h(k) + 2 = -\Gamma = -\left(2\gamma - 1 + \frac{1}{2\gamma - 1}\right). \tag{50}$$

or

$$\omega = kv = \pm\sqrt{\Gamma + 4 - 2\cos k}. \tag{51}$$

For given $\gamma > 1$ and $v > 0$, this dispersion relation has a number of roots

$$\begin{aligned} k &= \pm k_{2v+1} + i0 \quad (\text{for } v \geq 0), & k &= \pm k_{2v} - i0 \quad (\text{for } v > 0), \\ v &= 0, 1, \dots, N, \end{aligned} \tag{52}$$

where $N = 0$ if the speed is high enough; N increases as v decreases. Note that the waves (47) with $k = k_\mu$ and $k = -k_\mu$ form a real sinusoidal wave. Wavenumbers k_{2v-1} belong to waves whose phase velocity is greater than the group velocity, while an inverse relation is valid for k_{2v} -waves.

For $\gamma > 1$ the dispersion relation in Eq. (50) completely coincides with that corresponding to a pole of $\mathcal{L}(k)$, that is, it is equivalent to the equation $\gamma L(k) + 1 - \gamma = 0$. Thus, for $\gamma > 1$ a localized tail wave or (living aside the admissibility question in the sense of Section 4.7) several such waves can propagate behind the transition front with a constant (η -independent) amplitude. The wave amplitude and the wavenumber are defined by the solution (39) for $\theta_-(k)$, while its structure is defined in Eqs. (47)–(50) with $\lambda = \lambda_1$. In this wave, the energy flux relatively the transition front is directed along the transition line to $\eta = -\infty$.

4.4.1. Resonant waves

Two or three roots from Eq. (52) can unite. The positive double root is that of

$$(k - k_{2v-1} - i0)(k - k_{2v} + i0) \quad (k_{2v} = k_{2v-1}), \tag{53}$$

while the positive triple root corresponds to

$$(k - k_{2v-1} - i0)(k - k_{2v+1} - i0)(k - k_{2v} + i0) \quad (k_{2v-1} = k_{2v+1} = k_{2v}). \tag{54}$$

(The same, but negative roots also exist.) These wavenumbers correspond to resonant waves whose group and phase velocities coincide. In the considered phase transition problem where $\gamma > 1$ at $\eta < 0$, but not ahead of the transition front, only the ‘odd wavenumbers’ are important (others do not belong to $\mathcal{L}_-(k)$). So, in this case, the resonant wave corresponds only to the triple root that gives rise to the second-order pole of $\mathcal{L}_-(k)$.

For the triple root three equations are valid: Eq. (50) and two successive derivatives of it

$$\begin{aligned} kv^2 &= \sin k, \\ v^2 &= \cos k. \end{aligned} \tag{55}$$

The corresponding values of the wave number, the phase velocity (that coincides with the transition front velocity) and γ follows from these equations as

$$\begin{aligned} \sin k &= \frac{k}{\sqrt{k^2 + 1}} \Rightarrow k \approx \pm \left[(2\mu + 1/2)\pi - \frac{1}{(2\mu + 1/2)\pi} \right], \quad \mu = 1, 2, \dots, \\ v &= (k^2 + 1)^{-1/4}, \\ \gamma &= \frac{1}{2} + \frac{1}{4} (\Gamma + \sqrt{\Gamma^2 - 4}), \quad \Gamma = \frac{k^2 + 2}{\sqrt{k^2 + 1}}. \end{aligned} \tag{56}$$

Thus, there exists a set of special values of γ where, in the phase transition problem, the localized resonant waves are possible. For each such value only one real resonant wave is possible and it corresponds to only one value of v . The resonant parameters begin from

$$k \approx \pm 7.725, \quad v \approx 0.358, \quad \gamma \approx 2.322. \tag{57}$$

Then, when the resonant wavenumbers increase, the resonant speeds decrease and the corresponding values of γ increase. In the considered steady-state regime, the resonant wave amplitude is infinite. So, it corresponds to $G^0 = \infty$. If γ and v are not equal but close to their resonant values, the solution exists, but G^0 is large.

4.5. The limit at $\gamma = 1$

Eq. (38) has a limiting expression for $\gamma \rightarrow 1$. In this case

$$\begin{aligned} \text{Arg } \mathcal{L} &= \arctan \frac{(1 - \gamma)\Im L}{\gamma|L|^2 + (1 - \gamma)\Re L} \sim (1 - \gamma) \frac{\Im L}{|L|^2} = -(1 - \gamma)\Im \left(\frac{1}{L} \right), \\ \mathcal{R} &\sim 1 - \frac{1 - \gamma}{\pi} \int_0^\infty \Im \left[\frac{1}{L(k)} \right] \frac{dk}{k} \end{aligned} \tag{58}$$

and in the limit Eq. (38) becomes

$$\frac{1}{2} - \frac{1}{\pi} \int_0^\infty \Im \left[\frac{1}{L(k)} \right] \frac{dk}{k} = \frac{\theta_*}{P_*} = \frac{1}{1 + \sqrt{1 + 2G^0}} \tag{59}$$

with

$$G^0 = \frac{G}{\theta_*^2}, \quad G = \frac{1}{2} P_*^2 - P_* \theta_*. \tag{60}$$

Below this result will be obtained directly for $\gamma = 1$.

4.6. Discussion

The dependencies of $1/G^0$ on the wave speed, v , for some values of γ [see Eqs. (45) and (35)] are plotted in Fig. 6. The lower boundary of G^0 as a function of γ is presented in Fig. 7.

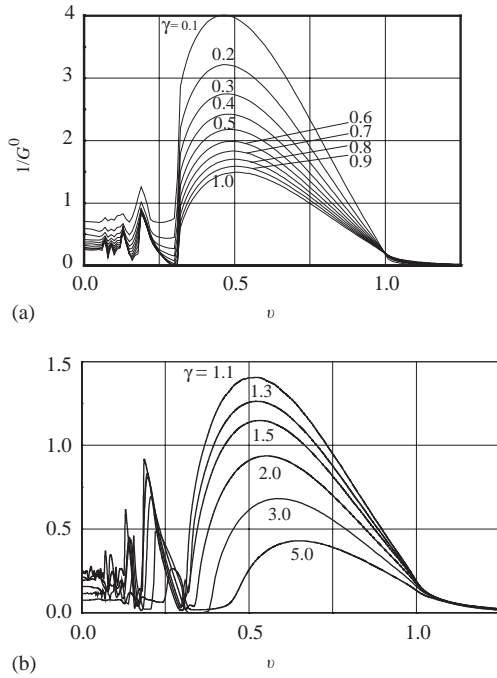


Fig. 6. The normalized energy release rate versus the transition wave speed for mode III of the square-cell lattice: (a) $\gamma \leq 1$; (b) $\gamma > 1$.

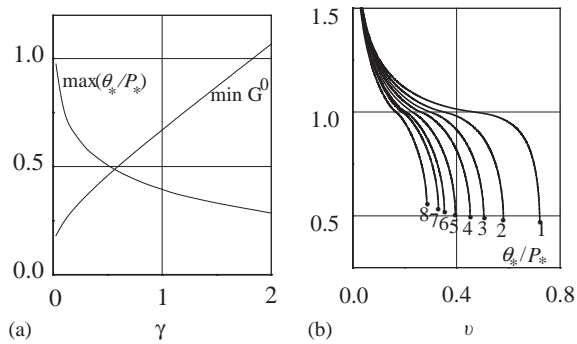


Fig. 7. (a) The lower boundary of the energy release rate, G^0 , and the upper boundary of the critical elongation, θ_*/P_* . (b) The right (admissible) branch of the speed as a function of θ_*/P_* . The lower boundary of the admissible speed is marked by bullets. Curves 1–8 correspond to $\gamma = 0.1, 0.3, 0.5, 0.7, 1.0, 1.3, 1.5$ and 2.0 , respectively.

It is seen that G^0 reaches its minimum roughly at $v=0.5$. After this, G^0 monotonically grows as v grows. This branch corresponds to admissible speeds (see Section 4.7), but the left branch does not. The value of the lower boundary, $v \approx 0.5$, is defined by the

dynamic amplification factor [see Slepyan, 2000, 2002, where it is shown that there is a lower boundary of the transition speed in an elastic system]. After the transition occurs in a front bond, under a small speed, the bond elongation approaches the final value oscillating relatively it. Let τ be the time required for the elongation to reach maximum. Roughly, it is equal to a half-period of the oscillations. If $v < 1/\tau$ is assumed, the next bond transition occurs under the elongation lower than the maximal one. This means that the elongation ahead the transition front exceeds the critical value, and hence this speed is not admissible. Otherwise, if $v \geq 1/\tau$, the speed is admissible since $q < q_*$ at $\eta > 0$. The lower boundary, $v \approx 0.5$, corresponds to the oscillation frequency of a unit mass supported by two–three unit-stiffness bonds. Among these bonds the second-phase, higher-stiffness bond plays a role, and it is seen that the lower speed boundary, $v = 1/\tau$, increases as γ increases, as it should be since an increase in the stiffness leads to a decrease in τ .

In the low-speed region, $v < 0.3$, more and more sinusoidal waves arise as the speed decreases. The intensity of each wave after its origin appears extremely sensitive to the speed. This causes irregularities in the dependencies shown in Fig. 6. As $v \rightarrow 0$, the number of such waves tends to infinity and the amplitude of the oscillations tends to zero.

4.7. Criterion of admissibility

In addition to the condition (3) [or, equivalently, $\theta(0) = \theta_*$], the analytical solution must be admissible in the sense that the bond elongation in the initial phase must be below the critical value, i.e. $\theta < \theta_*$ at $\eta > 0$. This condition also concerns all the bonds outside the transition line. Otherwise, the considered single-line steady-state transition wave does not exist. This condition is similar to that in fracture of lattices (Marder and Gross, 1995). In this connection, consider a necessary condition as

$$\frac{d\theta(\eta)}{d\eta} \leq 0 \quad (\eta = 0). \tag{61}$$

In terms of the Fourier transform, this derivative can be expressed as

$$\frac{d\theta(\eta)}{d\eta} = \lim_{k \rightarrow i\infty} (-ik)[(-ik)\theta_+(k) - \theta(0)] = \lim_{k \rightarrow -i\infty} (-ik)[ik\theta_-(k) - \theta(0)]. \tag{62}$$

Not that the derivative is continuous. To find this limit consider the Cauchy type integral in (33) where

$$\Re \ln \mathcal{L}(-k) = \Re \ln \mathcal{L}(k),$$

$$\Im \ln \mathcal{L}(-k) = -\Im \ln \mathcal{L}(k),$$

$$\Re \ln \mathcal{L}(k) = O\left(\frac{1}{k^2}\right) \quad (k \rightarrow \infty),$$

$$\Im \ln \mathcal{L}(k) = 0 \quad (k > \sqrt{8}/v). \tag{63}$$

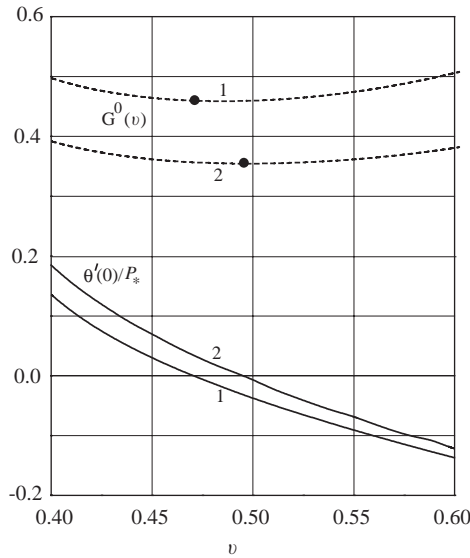


Fig. 8. The admissibility criterion: G^0 and $\theta'(0)/P_*$ [$\theta'(0) = d\theta(\eta)$ at $\eta = 0$] as functions of the speed: (1) $\gamma = 0.5$, (2) $\gamma = 1.5$. The minimal values of G^0 are marked by bullets.

These properties are enough for the estimation as

$$\int_{-\infty}^{\infty} \frac{\ln \mathcal{L}(\xi)}{\xi - k} dk = -\frac{2}{k} \int_0^{\infty} \ln |\mathcal{L}(\xi)| d\xi + o\left(\frac{1}{k}\right) \quad (k \rightarrow \pm i\infty). \tag{64}$$

Thus

$$\mathcal{L}_{\pm}(k) \sim 1 \pm \frac{i}{\pi k} \int_0^{\infty} \ln |\mathcal{L}(\xi)| d\xi \quad (k \rightarrow \pm i\infty). \tag{65}$$

Referring to Eqs. (35), (39) and (62) we now find the following expression:

$$\frac{d\theta(0)}{d\eta} = \frac{\mathcal{R}}{\pi\sqrt{\gamma}} \left(\frac{P_*}{\gamma - 1} + \theta_* \right) \int_0^{\infty} \ln |\mathcal{L}(\xi)| d\xi. \tag{66}$$

This result can be directly used if $\gamma \neq 1$, while the expression for $\gamma = 1$ can be obtained as the limit, $\gamma \rightarrow 1$, or directly from Eq. (72); it is

$$\frac{d\theta(0)}{d\eta} = -\frac{P_*}{\pi} \int_0^{\infty} \left[1 - \Re \frac{1}{L(k)} \right] dk, \tag{67}$$

where $L(k)$ is defined in Eqs. (16) and (19). Note that for $v > 0$ the considered integrals converge. The calculation results presented in Fig. 8 evidence that criterion (61) is satisfied for the stable branch of the speed–energy release rate dependence (where $dG^0/dv \geq 0$) and is not satisfied otherwise.

5. Parallel branches: $\gamma = 1$

5.1. Elastic lattice

Such a bistable model is remarkable for the fact that the transition from the one branch to the other does not change the left-hand side of the equation. It results only in self-equilibrated pairs of external forces applied to the particles connected by the corresponding bond, Fig. 3. These forces are independent of the elongation now. Thus, an intact uniform lattice can be considered, and only the right-hand side of the dynamic equation (which is independent of the lattice displacements) reflects the transition. This simplifies greatly the problem considered. Namely, it is no longer a mixed boundary value problem. Besides, in this case the superposition is valid allowing multiple transition bands to be considered.

In this case, Eq. (11) defines the elongation in the explicit form

$$\theta^F(k) = \frac{P_* Q^F}{0 + ik} = \frac{P_*}{0 + ik} \left[1 - \frac{1}{L(k)} \right]. \tag{68}$$

Note that in terms of the dimensional values

$$\theta^F(k) = \frac{P_*}{\mu(0 + ik)} \left[1 - \frac{1}{L(k)} \right]. \tag{69}$$

Further, since

$$\Re L(-k) = \Re L(k), \quad \Im L(-k) = -\Im L(k), \quad 1/L(0) = 0, \quad L(\pm\infty) = 1, \tag{70}$$

the inverse transform

$$\theta(\eta) = \frac{1}{2\pi} \int_{-\infty}^{\infty} \theta^F(k) e^{-ik\eta} dk \tag{71}$$

leads to the following result:

$$\begin{aligned} \theta(\eta) &= \left(\frac{1}{2} - I_1 - I_2 \right) P_* \\ I_1 &= \frac{1}{\pi} \int_0^{\infty} \Im \left[\frac{1}{L(k)} \right] \frac{\cos(k\eta)}{k} dk \rightarrow 0 \quad (\eta \rightarrow \infty), \\ I_2 &= \frac{1}{\pi} \int_0^{\infty} \left[1 - \Re \frac{1}{L(k)} \right] \frac{\sin(k\eta)}{k} dk = \begin{cases} 0 & (\eta = 0), \\ \pm \frac{1}{2} & (\eta = \pm\infty), \end{cases} \end{aligned} \tag{72}$$

where the first term, $\frac{1}{2}$, in the expression for $\theta(\eta)$ is a half-residue at $k = 0$. It follows that

$$\theta(0) = P_* \left\{ \frac{1}{2} - \frac{1}{\pi} \int_0^{\infty} \Im \left[\frac{1}{L(k)} \right] \frac{dk}{k} \right\}, \quad \theta(\infty) = 0, \quad \theta(-\infty) = P_*. \tag{73}$$

We thus come to the above limiting results, Eqs. (37), (58) and (40) [recall that $\theta(0) = \theta_*$ and if $\gamma = 1$ then $P_{**} = P_*$].

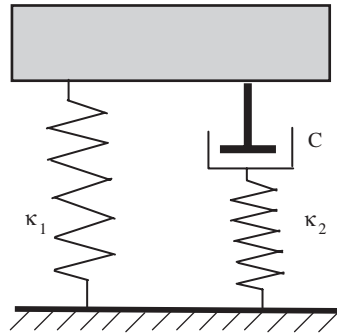


Fig. 9. The standard viscoelastic material unit.

5.2. Viscoelastic lattice

For this special type of the force-elongation diagram, if the branches differ only by the ‘elastic part’ of the tensile force (as discussed below), the elastic–viscoelastic correspondence principle is valid.

In an initial range of the extension, the bonds are assumed now to satisfy the standard material viscoelastic relation:

$$T + \beta \frac{dT}{dt} = \mu \left(q + \alpha \frac{dq}{dt} \right), \tag{74}$$

where α and β are the creep and relaxation times, respectively. For convenience we here preserve the dimension values. This relation corresponds to a unit presented in Fig. 9, where the left spring stiffness is κ_1 , the right spring stiffness is κ_2 and the viscous resistance of the element successively connected with the right spring is C . In these terms

$$\mu = \kappa_1, \quad \alpha = \frac{C}{\kappa_1} + \frac{C}{\kappa_2}, \quad \beta = \frac{C}{\kappa_2}. \tag{75}$$

Note that relation (74) can also be represented in the form

$$T = \frac{\mu}{\beta} e^{-t/\beta} \int_{-\infty}^t \left[q(\tau) + \alpha \frac{dq(\tau)}{d\tau} \right] e^{\tau/\beta} d\tau. \tag{76}$$

When the elongation reaches the critical value, q_* , the left spring is assumed to slip by a fixed value, such that its elongation becomes $q - q_{**}$, where q remains to be the elongation of the unit and

$$\kappa_1 q_{**} = \mu q_* = P_* = \text{const}. \tag{77}$$

It is assumed that

$$P_* \leq \mu q_*, \tag{78}$$

that is, the tensile force in the left spring remains nonnegative. Thus, after this transformation the stress–strain relation (76) becomes

$$T = \frac{\mu}{\beta} e^{-t/\beta} \int_{-\infty}^t \left[q(\tau) + \alpha \frac{dq(\tau)}{d\tau} \right] e^{\tau/\beta} d\tau - P_* \tag{79}$$

We assume that the initial state is well established and hence viscosity influences only the additional elongation caused by the transform. In accordance with the elastic–viscoelastic principle (or directly from Eq. (74)), the viscoelastic solution can be obtained from the elastic one (69) if μ is changed to the complex modulus μE with

$$E = \frac{1 + ikV_\alpha}{1 + ikV_\beta}, \quad V_\alpha = \frac{v\alpha}{a}, \quad V_\beta = \frac{v\beta}{a} \tag{80}$$

Accordingly, the function Y (18) must be replaced by

$$Y = \frac{(0 + ikv)^2}{E} \tag{81}$$

Formula (73) for the nondimensional elongation, $\theta(0)$, additional to the initial one becomes

$$\theta(0) = P_* \left\{ \frac{\beta}{2\alpha} - \frac{1}{\pi} \int_0^\infty \Im \left[\frac{1}{EL(k)} \right] \frac{dk}{k} \right\} \tag{82}$$

5.2.1. Massless viscoelastic lattice

This model relates to a very low transition speed that can be realized under the influence of viscosity (as in the case of a crack, see Slepyan et al., 1999; Slepyan, 2000, 2002). If the inertia term is neglected, $L(k)$ becomes a real periodic function and the equality $L(\pm\infty) = 1$ in Eq. (70) does not hold. We should return to Eq. (68) which for the considered massless viscoelastic lattice gives us

$$\theta^F(k) = \frac{P_*}{(0 + ik)E} \left[1 - \frac{1}{L(k)} \right] \tag{83}$$

with $Y = 0$. In this case, if $\beta > 0$ the elongation is discontinuous at $\eta = 0$ as follows directly from the behavior of the viscoelastic unit under discontinuous loading.

The inverse transform for $\eta = \pm 0$ can be represented as a sum of three terms. The first, as a half-residue at $k = 0$, is equal to $\frac{1}{2}$, the second is

$$\begin{aligned} & -\frac{P_*}{2\pi} \int_{-\infty}^\infty \frac{1 + ikV_\beta}{1 + ikV_\alpha} \left[1 - \frac{1}{L(k)} \right] \frac{\sin k\eta}{k} dk \\ & = \mp \frac{P_*}{2\pi} \int_{-\infty}^\infty \frac{1 + ikV_\beta/|\eta|}{1 + ikV_\alpha/|\eta|} \left[1 - \frac{1}{L(k/|\eta|)} \right] \frac{\sin k}{k} dk \\ & \rightarrow \mp \frac{P_*\beta}{2\alpha} (1 - \langle 1/L \rangle) \quad (\eta \rightarrow \pm 0), \end{aligned} \tag{84}$$

where $\langle 1/L \rangle$ is the averaged value of this periodic function, and the third can be written as

$$\begin{aligned}
 & -\frac{P_*}{2\pi} \int_{-\infty}^{\infty} \frac{1 - \beta/\alpha}{1 + k^2} \left[1 - \frac{1}{L(k/V_\alpha)} \right] \cos(k\eta/V_\alpha) dk \\
 & \rightarrow -\frac{P_*}{2} \left(1 - \frac{\beta}{\alpha} \right) \left[1 - \frac{2}{\pi} \int_0^\infty \frac{dk}{(1 + k^2)L(k/V_\alpha)} \right] \quad (\eta \rightarrow \pm 0). \tag{85}
 \end{aligned}$$

It follows that

$$\theta(\pm 0) = P_* \left\{ \frac{\beta}{2\alpha} [1 \mp (1 - \langle 1/L \rangle)] + \left(1 - \frac{\beta}{\alpha} \right) \frac{1}{\pi} \int_0^\infty \frac{dk}{(1 + k^2)L(k/V_\alpha)} \right\}. \tag{86}$$

For the square-cell lattice it is

$$\langle 1/L \rangle = \frac{1}{\pi} \int_0^\pi \frac{\sin k/2}{\sqrt{1 + \sin^2 k/2}} dk = \frac{1}{2}, \tag{87}$$

while for modes I and II triangular-cell lattice it is approximately equal to $\frac{1}{3}$.

The limiting values of the integral in Eq. (86) are

$$\frac{1}{\pi} \int_0^\infty \frac{dk}{(1 + k^2)L(k/V_\alpha)} \rightarrow \begin{cases} \frac{1}{2} \langle 1/L \rangle & (V_\alpha \rightarrow 0) \\ 0 & (V_\alpha \rightarrow \infty). \end{cases} \tag{88}$$

Regarding the limit for $V_\alpha \rightarrow \infty$ it is assumed that v remains well below the elastic wave speed, c , not to contradict the quasi-static formulation. This can be possible if $C_\alpha = \alpha c/a \gg \gg 1$.

Note that the relation

$$\theta(+0) = \theta_* \tag{89}$$

must be used now. This relation has the following limiting expressions:

$$\begin{aligned}
 \theta(+0) &= \frac{P_*}{2} \langle 1/L \rangle = \theta_* \quad (V_\alpha = 0), \\
 \theta(+0) &= \frac{\beta P_*}{\alpha} \langle 1/L \rangle = \theta_* \quad (V_\alpha = \infty). \tag{90}
 \end{aligned}$$

It can be seen that the resistance to the propagation of the considered localized wave, that is, the required value of P_* , increases with its speed in an initial range of the speed. This increase is most pronounced for small ratios β/α . For $\beta = 0$, $\alpha > 0$ the resistance tends to infinity when $V_\alpha \rightarrow \infty$. Such a boundary layer type of the solution is similar to that obtained for the quasi-static crack growth in a viscoelastic lattice (Slepyan et al., 1999). This solution evidences that a stable region, where $q(0)$ decreases as the speed increases, does exist if $\beta/\alpha < 1$. This conclusion, however, is based on the quasi-static formulation, which is valid if the viscosity times fall into the heart of the static-amplitude-response domain; that is, if $\alpha c/a$ is large enough, while β/α is small (see Slepyan, 2000, 2002).

Note that in the elastic case ($\alpha = \beta$)

$$\theta(0) = \frac{P_*}{2} \langle 1/L \rangle \quad (91)$$

for any v and hence the quasi-static regime corresponds to the initial elongation

$$q_0 = q_* - \frac{P_*}{2} \langle 1/L \rangle. \quad (92)$$

5.3. Transient problems

Numerical simulations are conducted for transient processes related to the above-considered steady-state problem for the square-cell bistable-bond lattice. The lattice nondimensional equations

$$\frac{d^2 u_{m,n}}{dt^2} = T_{m+1,n}^g - T_{m,n}^g + T_{m,n+1}^v - T_{m,n}^v \quad (93)$$

are considered, where $T_{m,n}^g$ is the tensile force in the bond connecting the particles m, n and $m-1, n$, while $T_{m,n}^v$ is the tensile force in the bond connecting the particles m, n and $m, n-1$. Initially the vertical bonds are stressed, while the horizontal bonds are not. As a result, the force-elongation dependence for the additional deformation appears different for these two families of the bonds, namely

$$T^g = \theta \quad (t < t_g), \quad T^g = \gamma\theta - P_{**} \quad (t > t_g);$$

$$T^v = \theta \quad (t < t_v), \quad T^v = \gamma\theta - P_{**} \quad (t > t_v);$$

$$t < t_g: \theta < q_*, \quad t = t_g: \theta = q_*,$$

$$t < t_v: \theta < \theta_*, \quad t = t_v: \theta = \theta_* < q_*. \quad (94)$$

The ratios q_*/θ_* and θ_*/P_* are the main input parameters. Note that the ratio, q_*/θ_* , is the safety factor for the horizontal bonds. In other respect, only the latter ratio, θ_*/P_* , is important.

We consider the domain $|m| \leq m_{\max}, |n| \leq n_{\max}$, where m_{\max} and n_{\max} are chosen such that the waves reflected from the boundaries do not reach the domain of interest. Initially the lattice is at rest with $\theta = 0$. To set it in motion, at the initial moment, $t = 0$, we give the velocity w to the particles $n = 0, |m| \leq 2$ and the velocity $-w$ to the opposite particles, $n = -1, |m| \leq 2$, —as the initial disturbance. Note that an increase in the number of the excited particles in these lines does not influence the wave parameters. The initial particle velocity, w , is set beginning from the minimal value of w , $w = w_*(\theta_*/P_*)$, which is enough to initiate the propagating transition wave, and to $w = (2 \div 3)w_*$.

The results of numerical simulations show that the transition wave does propagate along a single line if (a) the energy release rate is not too large, $G^0 < 5.26$ ($\theta_*/P_* > 0.228$) [in this case, the transition wave speed is subsonic, $v < 1$] and (b) the initial disturbance is low enough. Otherwise, a multiple-line wave propagates. In this latter case, the wave fronts in different lines appear shifted relatively each other. Note that

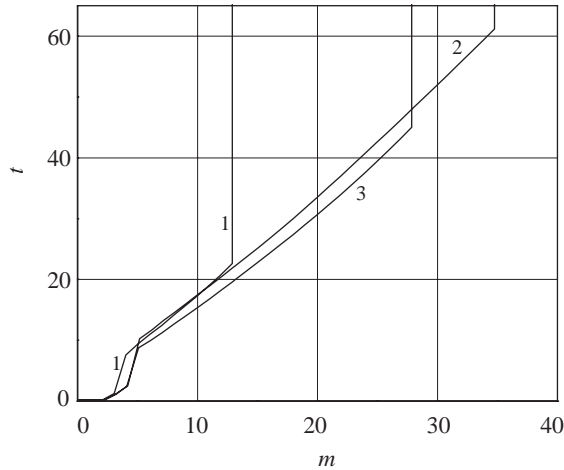


Fig. 10. Transitions under a low-energy release rate, $G^0 = 0.625$ ($\theta_*/P_* = 0.4, w_* = 1.215$): (1) $w = w_*$, (2) $w = 1.5$, (3) $w = 1.75$.

the energy release rate defines the sinusoidal waves intensity, and if it is large enough these waves cause the multiple-line transition—in the same way as a strong initial disturbance causes that.

In the single-line case, a good coincidence of the transition wave speeds found analytically, v_a , and numerically, v_c , is found. Note that the right (stable) branch of the multivalued function $v(G^0)$, Fig. 6, is taken into account. The minimal value of the energy release rate, G_{\min}^0 , of which the steady-state transition wave exists, is $G_{\min}^0 \approx 0.670$ ($\theta_*/P_* \approx 0.395$); the corresponding speed is $v_a \approx 0.508$.

For the normalized energy release rate less than ≈ 0.670 the steady-state solution does not exist, while some finite disturbance-level-dependent regions of the transition are found numerically. In Fig. 10, the lines interconnect the discrete points in which the transition front arrives to the bonds numbered by m (here and below in figures of this type the wave front propagation is shown for the first quarter of the lattice). The results correspond to the bonds $n=0, -1$ and to various w , beginning from $w = w_* = 1.215$.

Results of calculations in Fig. 11 correspond to $G^0 = 4$ ($\theta_*/P_* = 0.25, w_* \approx 0.271$) and $w = 0.5$. In this case, the transition incorporates six additional lines above the main one (and also six lines below it). In contrast, the dashed line corresponds to $w = w_*$, where only a single-line wave arises. As can be seen in Fig. 11 the multiple-line wave speed (the same for each line) is somewhat lower than that for the single-line wave. It is of interest to note that the transition in a line can arise not only at central bonds, $|m| \leq 2$, but also in several bonds with $|m| > 2$ (these points are the local minima of the curves).

The results for supersonic wave speed are presented in Fig. 12 where the transition in several lines is shown. In fact, the transition occurs in each line of the considered lattice strip in this regime. However, in the supersonic regime, the numerically

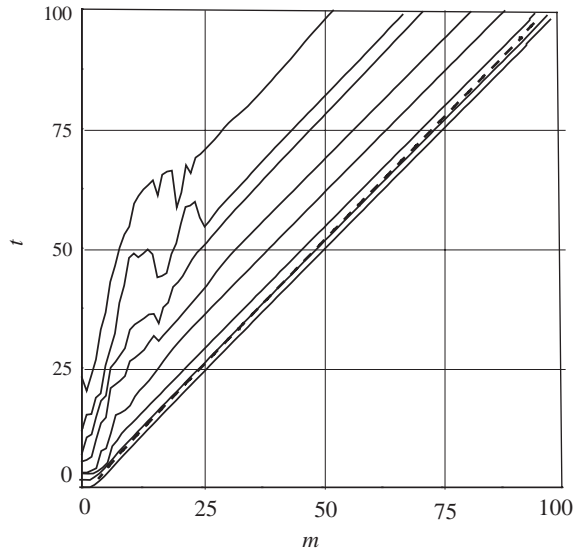


Fig. 11. Subsonic transitions, $G^0 = 4$ ($\theta_*/P_* = 0.25$, $w_* \approx 0.271$). From the bottom: the bond lines between $n = -1, 0, 1, \dots, 7$ are shown by solid lines for $w = 0.5$. The dashed line corresponds to a single-line transition wave obtained in the numerical simulations.

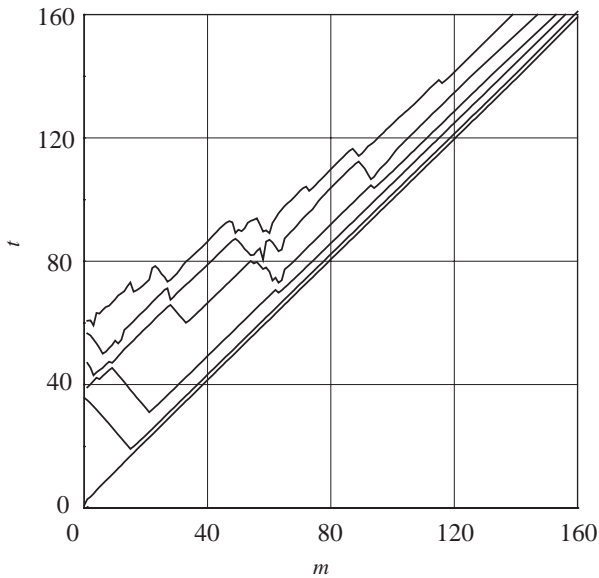


Fig. 12. Supersonic transitions, $G^0 = 7.5$ ($\theta_*/P_* = 0.2$), $w = 0.172$. From the bottom: the bond lines between $n = -1, 0, 1, \dots, 5$ are shown.

determined transition wave speed coincides with that obtained analytically for a single-line transition.

6. Continuous elastic model

It is of interest to consider the localized transition wave in the framework of the continuous material model. The related steady-state problem for a continuous elastic medium can be formulated as that for the upper half-plane, $y > 0$, with the following boundary conditions at $y = 0$ for modes I, II, and III, respectively:

$$\sigma_{xy} = 0 \quad (-\infty < \eta < \infty), \quad \sigma_{yy} = -P_{**} + \kappa u_y \quad (\eta < 0), \quad u_y = 0 \quad (\eta > 0), \quad (95)$$

$$\sigma_{yy} = 0 \quad (-\infty < \eta < \infty), \quad \sigma_{yx} = -P_{**} + \kappa u_x \quad (\eta < 0), \quad u_x = 0 \quad (\eta > 0), \quad (96)$$

$$\sigma_{yz} = -P_{**} + \kappa u_z \quad (\eta < 0), \quad u_z = 0 \quad (\eta > 0). \quad (97)$$

This formulation is the same as that for a crack at $\eta < 0$ whose faces are loaded by the above-expressed traction. So, the traction corresponds to the crack faces' interaction in the second phase of the initially stressed material—similarly to that shown in Fig. 2. Also, the energy criterion for the transition is used as in the case of a crack, namely, we assume that the transition occurs when the energy release rate at the moving point, $\eta = 0$, is critical

$$G = G_c. \quad (98)$$

To solve these problems we can use the corresponding results for the steady-state crack dynamics (see e.g. Slepyan, 2002, formulas (9.83)–(9.87)) with the crack face traction defined in the relations (95)–(97) for $\eta < 0$. In this way, we obtain the governing equation as

$$L(k)\sigma_+ + u_- = \frac{P_{**}L(k)}{0 + ikv} \quad (99)$$

with

$$L(k) = \left[\kappa + \frac{\mu\sqrt{(0 + ik)(0 - ik)}}{(1 - \nu)D_0(v)} \right]^{-1}, \quad (100)$$

where μ is the shear modulus, ν is the Poisson's ratio (for mode III it must be taken $\nu = 0$) and for subcritical speeds

$$D_0(v) = -\frac{v^2\sqrt{1 - v^2/c_1^2}}{(1 - \nu)c_2^2R(v)} \quad (\text{mode I}),$$

$$D_0(v) = -\frac{v^2\sqrt{1 - v^2/c_2^2}}{(1 - \nu)c_2^2R(v)} \quad (\text{mode II}),$$

$$D_0(v) = \frac{1}{\sqrt{1 - v^2/c_2^2}} \quad (\text{mode III}), \quad (101)$$

where $R(v)$ is the Rayleigh function and $c_{1,2}$ are the longitudinal and shear wave speeds, respectively.

We now introduce a normalized function as

$$L^0(k) = \lambda(k)L(k), \quad \lambda(k) = \frac{\mu\sqrt{(0+ik)(0-ik)}}{(1-\nu)D_0(v)}. \tag{102}$$

This function satisfies the conditions

$$L^0(k) \rightarrow 1 \quad (k \rightarrow \pm\infty), \quad \text{Ind } L^0(k) = 0 \tag{103}$$

required for the use of the Cauchy type integral for the factorization. As a result, we have

$$\begin{aligned} L(k) &= L_+(k)L_-(k), \quad L_{\pm}(k) = L_{\pm}^0(k)/\lambda_{\pm}(k), \\ L_{\pm}^0(k) &= \exp \left[\pm \frac{1}{2\pi i} \int_{-\infty}^{\infty} \frac{\ln L^0(\xi)}{\xi - k} d\xi \right] \quad (\pm \Im k > 0), \\ \lambda_{\pm}(k) &= \sqrt{\frac{\mu(0 \mp ik)}{(1-\nu)D_0(v)}}. \end{aligned} \tag{104}$$

The factors have the following asymptotes:

$$\begin{aligned} L_{\pm}^0(k) &\rightarrow 1 \quad (k \rightarrow \pm i\infty), \\ L_{\pm}(k) &\sim \sqrt{\frac{(1-\nu)D_0(v)}{\mu(0 \mp ik)}}, \\ L_{\pm}(0) &= \frac{1}{\sqrt{\kappa}}. \end{aligned} \tag{105}$$

Eq. (99) can now be represented as

$$L_+(k)\sigma_+ + \frac{u_-}{L_-(k)} = \frac{P_{**}[L_+(k) - L_+(0)]}{0 + ik} + \frac{P_{**}L_+(0)}{0 + ik}. \tag{106}$$

The first terms in the left- and right-hand sides are regular in the upper half-plane k with the real axis, while the second terms are regular in the lower half-plane with its boundary. This allows us to write down the required solution as

$$\begin{aligned} \sigma_+ &= \frac{P_{**}}{0 + ik} \left[1 - \frac{1}{\sqrt{\kappa}L_+(k)} \right] \sim \frac{P_{**}}{\sqrt{s}} \sqrt{\frac{\mu}{\kappa(1-\nu)D_0(v)}} \quad (k = is, s \rightarrow \infty), \\ u_- &= \frac{P_{**}}{\sqrt{\kappa}(0 + ik)} L_-(k) \sim \frac{P_{**}}{s^{3/2}} \sqrt{\frac{(1-\nu)D_0(v)}{\mu\kappa}} \quad (k = -is, s \rightarrow \infty). \end{aligned} \tag{107}$$

The energy release rate at the moving transition point, $\eta = 0$, can be calculated as for a crack (see Slepyan, 2002, formula 1.42). In our case, the total energy release

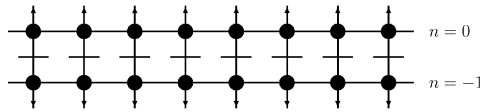


Fig. 13. The one-layer lattice strip as a version of Frenkel–Kontorova model. Due to symmetry of the structure and the prestress, only the upper half-strip can be considered with the vertical bonds fixed on the axis of symmetry shown by the dashed line. It is assumed that the vertical bonds obey the bistable force–elongation relation, while the horizontal bonds always remain in the initial phase—as in the case of the infinite two-dimensional lattice.

rate from the upper and the lower half-planes is thus

$$G = \lim_{s \rightarrow \infty} s^2 \sigma_+(is) u_-(-is) = \frac{P_{**}^2}{\kappa}. \tag{108}$$

This is nothing but the energy produced per unit length by the upper and lower crack face traction at $\eta < 0$, that is, by the crack faces’ interaction. Such a result could be expected from the beginning. Indeed, in the subcritical steady-state regime, there exist no waves which could carry energy away, and only the singular transition point can consume the produced energy. So, in contrast to that in the lattice, the energy release rate is speed-independent here, while the resulting energy release (as the produced energy, P_{**}^2/κ , minus G) is zero. Thus, this solution exists if the required energy, G_c , is exactly equal to the energy, G , produced by the traction.

What happens if the prestress of the elastic plane (which results in the considered ‘active’ type of the crack faces interaction) is greater than the critical one, that is, if $G > G_c$? In this case, in an elastic body, the steady-state regime does not exist, and the transition wave speed is not a constant, but asymptotically verges towards the critical value. In such a quasi-steady-state regime, there exists radiation energetically equal to the resulting energy release, $P_{**}^2/\kappa - G_0$. Thus the classical, homogeneous-body formulation leads to a very different result in comparison with that based on the lattice model where the steady-state regime exists for any, but not too small, resulting energy release rate, and the speed is energy-release-rate-dependent.

7. Related version of one-dimensional discrete Frenkel–Kontorova model

Consider a square-cell lattice strip consisting of one layer with bistable bonds connecting the particle lines $n=0$ and $n=-1$, Fig. 13. Due to symmetry the upper half-strip can be considered as a version of one-dimensional discrete Frenkel–Kontorova model (also see Kresse and Truskinovsky, 2004) where the particles are connected by bistable bonds with a rigid substrate. (Note that in the regular Frenkel–Kontorova model the force–displacement relation is multistable and reversible.)¹ The dynamic equation is

$$\ddot{u}_m(t) = u_{m-1}(t) + u_{m+1}(t) - 4u_m(t) + [P_* + (1 - \gamma)(2u_m(t) - \theta_*)]H(-\eta), \tag{109}$$

¹ See <http://monet.physik.unibas.ch/~elmer/flab/FKModel/>.

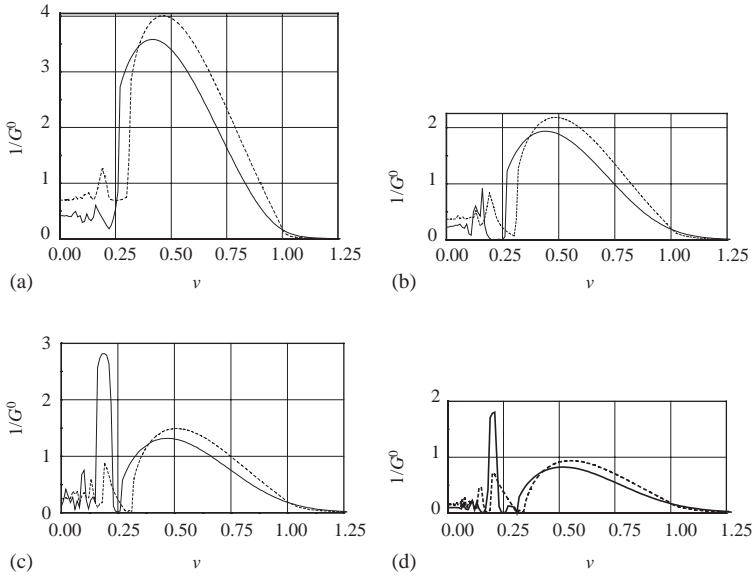


Fig. 14. The transition wave speed dependencies for the considered version of Frenkel–Kontorova model (solid curves) and the corresponding dependencies for the infinite lattice (dashed curves): (a) $\gamma = 0.1$, (b) $\gamma = 0.5$, (c) $\gamma = 1.0$, (d) $\gamma = 2.0$.

where $u_m(t)$ is the particle displacement. The governing relations (23)–(25), respective the Fourier transforms of $\theta(\eta) = 2u(\eta)$, follow from this with

$$\mathcal{L}(k) = \frac{h(k) + 2}{h(k) + 2\gamma} = \frac{L(k)}{\gamma L(k) + 1 - \gamma},$$

$$L(k) = L_{FK}(k) = \frac{h(k) + 2}{h(k)}, \quad h(k) = (0 + ikv)^2 + 2(1 - \cos k). \quad (110)$$

The solution to the chain problem differs from that obtained for the two-dimensional lattice only by the expression for the function $\mathcal{L}(k)$, because, as far as this function is obtained, the considerations concern only the transition-line bonds. The comparative results are presented in Fig. 14. It is seen that qualitatively the $1/G^0$ – ν dependencies for FK model are similar to those for the lattice. Quantitatively they are also not too far from each other, and only the low-speed ‘resonances’ are more pronounced in the case of the one-dimensional model. The basic differences are in the structure of the dissipative waves. The comparison thus evidences that the transition wave speed not too strongly depends on directions of the radiation; it mainly depends on the energy release rate and γ .

Acknowledgements

This research was supported by The Israel Science Foundation, Grant No. 28/00-3 and ARO Grants No. 41363-MA and No. 45584-MA.

References

- Balk, A.M., Cherkaev, A.V., Slepyan, L.I., 2001a. Dynamics of chains with non-monotone stress–strain relations. I. Model and numerical experiments. *J. Mech. Phys. Solids* 49, 131–148.
- Balk, A.M., Cherkaev, A.V., Slepyan, L.I., 2001b. Dynamics of chains with non-monotone stress–strain relations. II. Nonlinear waves and waves of phase transition. *J. Mech. Phys. Solids* 49, 149–171.
- Biner, S.B., 2002. Stress states and growth behavior of bridged cracks at creep regime. *Eng. Fract. Mech.* 69, 923–943.
- Budiansky, B., Hutchinson, J.W., Evans, A.G., 1986. Matrix fracture in fiber-reinforced ceramics. *J. Mech. Phys. Solids* 34, 167–189.
- Charlotte, M., Truskinovsky, L., 2002. Linear chains with a hyper-pre-stress. *J. Mech. Phys. Solids* 50, 217–251.
- Cherkaev, A., Cherkaev, E., Slepyan, L., 2004. Transition waves in bistable structures. I. Chains with a large gap between stable states, submitted.
- Fineberg, J., Marder, M., 1999. Instability in dynamic fracture. *Phys. Rep.* 313, 1–108.
- Fineberg, J., Gross, S.P., Marder, M., Swinney, H.L., 1991. Instability in dynamic fracture. *Phys. Rev. Lett.* 67 (4), 457–460.
- Fineberg, J., Gross, S.P., Marder, M., Swinney, H.L., 1992. Instability in the propagation of fast cracks. *Phys. Rev. B* 45 (10), 5146–5154.
- Frenkel, J., Kontorova, T., 1938. On the theory of plastic deformation and twinning. *Sov. Phys. JETP* 13, 1–10.
- Gerde, E., Marder, M., 2001. Friction and Fracture. *Nature* 413, 285–288.
- Huang, Y., Wang, W., Liu, C., Rosakis, A.J., 1999. Analysis of intersonic crack growth in unidirectional fiber-reinforced composites. *J. Mech. Phys. Solids* 47, 1893–1916.
- Kessler, D.A., 2000. Steady-state cracks in viscoelastic lattice models II. *Phys. Rev. E* 61 (3), 2348–2360.
- Kessler, D.A., Levine, H., 1998. Steady-state cracks in viscoelastic lattice models. *Phys. Rev. E* 59 (5), 5154–5164.
- Kessler, D.A., Levine, H., 2001. Nonlinear lattice models of viscoelastic mode III fracture, *Phys. Rev. E* 63 (1), 016118/1–9.
- Kresse, O., Truskinovsky, L., 2003. Mobility of lattice defects: discrete and continuum approaches. *J. Mech. Phys. Solids* 51 (7), 1305–1332.
- Kresse, O., Truskinovsky, L., 2004. Lattice friction for crystalline defects: from dislocation to cracks. *J. Mech. Phys. Solids*, submitted.
- Kulakhmetova, S.A., Saraikin, V.A., Slepyan, L.I., 1984. Plane problem of a crack in a lattice. *Mechanics of Solids* 19, 101–108.
- Marder, M., Liu, X., 1993. Instability in lattice fracture. *Phys. Rev. Lett.* 71 (15), 2417–2420.
- Marder, M., Gross, S., 1995. Origin of crack tip instabilities. *J. Mech. Phys. Solids* 43, 1–48.
- Meda, G., Steif, P.S., 1994a. A detailed analysis of cracks bridged by fibers—I. Limiting cases of short and long cracks. *J. Mech. Phys. Solids* 42, 1293–1321.
- Meda, G., Steif, P.S., 1994b. A detailed analysis of cracks bridged by fibers—II. Cracks of intermediate size. *J. Mech. Phys. Solids* 42, 1323–1341.
- Movchan, N.V., Willis, J.R., 1996. Critical load for a mode-I crack reinforced by fibres. *Quart. J. Mech. Appl. Math.* 49 (4), 545–564.
- Movchan, N.V., Willis, J.R., 1997a. Asymptotic analysis of reinforcement by frictional fibres. *Proc. R. Soc. A* 453, 757–784.
- Movchan, N.V., Willis, J.R., 1997b. Influence of spatial correlations on crack bridging by frictional fibres. *Eng. Fract. Mech.* 58, 571–579.

- Movchan, N.V., Willis, J.R., 1998. Penny-shaped crack reinforced by fibres. *Q. Appl. Math.* 56 (2), 327–340.
- Movchan, A.B., Bullough, R., Willis, J.R., 2003. Two-dimensional lattice models of the Peierls type. *Philos. Mag.* 83 (5), 569–587.
- Nekorkin, V.I., Velarde, M.G., 2002. Synergetic phenomena in active lattices. *Patterns, Waves, Solitons, Chaos*. Springer, Berlin.
- Nemat-Nasser, S., Luqun, N., 2001. A fiber-bridged crack with rate-dependent bridging forces. *J. Mech. Phys. Solids* 49, 2635–2650.
- Ngan, S.-C., Truskinovsky, L., 2002. Thermo-elastic aspects of dynamic nucleation. *J. Mech. Phys. Solids* 50, 1193–1229.
- Pechenik, L., Levine, H., Kessler, D.A., 2002. Steady-state mode I cracks in a viscoelastic triangular lattice. *J. Mech. Phys. Solids* 50, 583–613.
- Puglisi, G., Truskinovsky, L., 2000. Mechanics of a discrete chain with bi-stable elements. *J. Mech. Phys. Solids* 48, 1–27.
- Slepyan, L.I., 1981. Dynamics of a crack in a lattice. *Sov. Phys. Dokl.* 26, 538–540.
- Slepyan, L.I., 2000. Dynamic factor in impact, phase transition and fracture. *J. Mech. Phys. Solids* 48, 931–964.
- Slepyan, L.I., 2001a. Feeding and dissipative waves in fracture and phase transition. I. Some 1D structures and a square-cell lattice. *J. Mech. Phys. Solids* 49, 469–511.
- Slepyan, L.I., 2001b. Feeding and dissipative waves in fracture and phase transition. II. Phase-transition waves. *J. Mech. Phys. Solids* 49, 513–550.
- Slepyan, L.I., 2001c. Feeding and dissipative waves in fracture and phase transition. III. Triangular-cell lattice. *J. Mech. Phys. Solids* 49, 2839–2875.
- Slepyan, L.I., 2002. *Models and Phenomena in Fracture Mechanics*. Springer, Berlin.
- Slepyan, L.I., Ayzenberg-Stepanenko, M.V., 2002. Some surprising phenomena in weak-bond fracture of a triangular lattice. *J. Mech. Phys. Solids* 50 (8), 1591–1625.
- Slepyan, L.I., Troyankina, L.V., 1984. Fracture wave in a chain structure. *J. Appl. Mech. Techn. Phys.* 25 (6), 921–927.
- Slepyan, L.I., Troyankina, L.V., 1988. Shock waves in a nonlinear chain. In: Gol'dstein, R.V. (Ed.), *Plasticity and Fracture of Solids*. Nauka, Moscow, pp. 175–186 (in Russian).
- Slepyan, L.I., Ayzenberg, M.V., Dempsey, J.P., 1999. A lattice model for viscoelastic fracture. *Mech. Time-Dependent Mater.* 3, 159–203.
- Slepyan, L., Cherkaev, A., Cherkaev, E., 2004. Transition waves in bistable structures. II. Analytical solution: wave speed and energy dissipation. *J. Mech. Phys. Solids*, submitted.
- Truskinovsky, L., Vainchtein, A., 2004. Explicit kinetic relation from “first principles”. In: Ogden, R., Gao, D. (Eds.), *Mechanics of Material forces, Euromech 445, Advances in Mechanics and Mathematics*, Kluwer, Dordrecht, pp. 1–8.
- Willis, J.R., 1993. Asymptotic analysis of crack bridging by ductile fibres. *Composites* 24, 93–97.